DOI: 10.18721/JPM.13109
УДК 537.531, 621.371, 539.234

# NANOSTRUCTURED CARBON AND ORGANIC FILMS: SPECTRAL MICROWAVE AND OPTICAL CHARACTERISTICS

*V.V. Starostenko, A.S. Mazinov, A.S. Tyutyunik,*
*I.Sh. Fitaev, V.S. Gurchenko*

V.I. Vernadsky Crimean Federal University,
Simferopol, Republic of Crimea, Russian Federation

Microwave and optical transmission and reflection spectra of thin films prepared by casting the aqueous and dichloromethane solutions of fullerene, as well as casting the chloroform solution of 4-methylphenylhydrazone N-isoamylisatin have been recorded in the 2.5 – 4.0, 8.2 – 12.0 GHz and 19 – 110, 330 – 740 THz ranges. The carbon samples precipitated from dichloromethane were established to be the most sensitive to the microwaves. There were 3.4 and 9.1 GHz absorption peaks in their spectrum. The 20 – 50 and 78 – 108 THz IR intervals were chosen for investigation as the most pronounced. The fullerene-containing films, having a linear optical spectrum, exhibited the maximal absorption factor. The organic samples, having a sharp increase of optical absorption in the 599.6 – 713.8 THz. high-frequency region, exhibited an absorption edge of 3.05 eV. In this case the surface photomicrographs demonstrated a rather ramified relief with nontrivial 3D forms dependent on the solution nature, notably prominent for fullerene surfaces.

**Keywords:** electromagnetic microwaves, fullerene, organic film, optical range, photomicrograph

**Citation:** Starostenko V.V., Mazinov A.S., Tyutyunik A.S., Fitaev I.Sh., Gurchenko V.S., Nanostructed carbon and organic films: spectral microwave and optical characteristics, St. Petersburg Polytechnical State University Journal. Physics and Mathematics. 13 (1) (2020) 98–108. DOI: 10.18721/JPM.13109



# СПЕКТРАЛЬНЫЕ СВЧ- И ОПТИЧЕСКИЕ ХАРАКТЕРИСТИКИ НАНОСТРУКТУРИРОВАННЫХ УГЛЕРОДНЫХ И ОРГАНИЧЕСКИХ ПЛЕНОК

*В.В. Старостенко, А.С. Мазинов, А.С. Тютюник,*
*И.Ш. Фитаев, В.С. Гурченко*

Крымский федеральный университет имени В.И. Вернадского,
г. Симферополь, Республика Крым, Российская Федерация

Представлены спектры пропускания и отражения электромагнитного излучения для тонких пленок, полученных методом полива из растворов фуллеренов в воде и дихлорметане, а также из растворов 4-метилфенилгидразона N-изоамилизатина в хлороформе, в СВЧ- (2,5 4,0 – и 12,0 – 8,2 ГГц) и оптических (110 – 19 и 740 – 330 ТГц) диапазонах. Показано, что наиболее чувствительны к СВЧ-волнам углеродные образцы, осажденные из дихлорметана, на спектре которых отмечены пики поглощения 3,4 и 9,1 ГГц. В инфракрасном диапазоне были выделены частотные интервалы 20 – 50 и 78 – 108 ТГц, где наиболее ярко проявилось взаимодействие электромагнитных волн с образцами. В оптическом спектре пленки, полученные из двух видов фуллеренсодержащих суспензий, имея линейный спектр, обладали максимальным коэффициентом поглощения, а органические образцы с резким увеличением поглощения в высокочастотной области 713,8 – 599,6 ТГц имели край полосы поглощения 3,05 эВ. При этом микрофотографии поверхностей показали достаточно разветвленный рельеф (в особенности для поверхностей фуллерена) с нетривиальными 3D-образованиями, на форму которых влиял тип растворителя.

**Ключевые слова:** СВЧ электромагнитные волны, фуллерен, органическая пленка, оптический диапазон, микрофотография

**Ссылка при цитировании:** Старостенко В.В., Мазинов А.С., Тютюник А.С., Фитаев И.Ш., Гурченко В.С. Спектральные СВЧ- и оптические характеристики наноструктурированных углеродных и органических пленок // Научно-технические ведомости СПбГПУ. Физико-математические науки. 2020. Т. 13. № 1. С. 109–120. DOI: 10.18721/JPM.13109



## Introduction

New frequency ranges are introduced for modern radio transceivers, as efforts are made to reduce the sizes and weights of the devices, accompanied by steadily decreasing costs; as a result, the search continues for new materials that can effectively interact with electromagnetic radiation in different frequency ranges. Fiber-optic channels transmitting the largest amounts of data traffic [1] and microwave cellular stations providing direct communication with customers [2,3] remain the key communications today.

The interest towards nanostructured carbon derivatives (carbon nanotubes, graphenes, fullerenes) grew considerably in the late 1990s and early 2000s. These structures not only possess unique physical properties [4–6] but also exhibit broadband absorption in combination with other materials. [7, 8]. Using nanocomposites to construct elementary active devices [9] should make it easy to integrate organocarbon elements into existing electronic circuits of modern transceivers.

Combined with organic materials, these elements can serve as a basis for novel emitting [10] and diode structures [11, 12], significantly expanding their operating ranges.

However, such devices have certain drawbacks, primarily, photopolymerization (undesirable changes in properties induced by exposure to light), photostimulated and ordinary oxidation [13, 14] leading to rapid degradation of organic layers used.

Despite wide interest in organocarbon materials, their frequency properties are mainly used in the visible range, while their characteristics in the medium-wave infrared (IR) and microwave ranges are poorly studied.

In this study, we considered the effects of electromagnetic waves of microwave and optical ranges on nanostructured films of $C_{60}$ fullerene and N-isoamylisatin 4-methylphenylhydrazone (IMPH) organic precursor, serving as the main working layers of the corresponding heterojunctions [15].

## Measurement procedure and experimental samples

Since the initial studies focused on barrier structures [15], we considered the effect of electromagnetic radiation on thin films, i.e., on the type of matter from which these heterojunctions were made [12]. Examining $C_{60}$ and IMPH samples, we focused on measurements and analysis of reflection and transmission spectra of electromagnetic radiation in the microwave and optical ranges.

The microwave region was represented by two ranges: 2.5–4.0 and 8.2–12.0 GHz. Thin square substrates of two sizes, 18 × 18 and 6 × 6 mm, were prepared from the given materials for measurements on waveguides with cross sections of 72 × 34 and 23 × 10 mm, respectively.

Optical measurements were carried out in two frequency ranges: mid-wave infrared 19–110 THz (650–3650 cm$^{-1}$) and visible 330–740 THz (405–909 nm). Samples of the same size, 18 × 18 mm, were made for this purpose.

The $C_{60}$ samples were examined in two phase states. One of them was a fullerene-containing aqueous solution (fullerene water system (FWS)), which was 99.9% pure [16]. Another $C_{60}$ was a solid-phase powder obtained by sputtering graphite [17, 18], 99.5% pure.

The primary FWS suspension was synthesized from crystalline $C_{60}$ (20 mg subsample), dissolved in N-methylpyrrolidone (25 ml) using a magnetic stirrer. The resulting purple-brown solution was mixed with distilled water (12.5 to 100 ml). The resulting clear dark red solution was stirred for 1 h and subjected to exhaustive dialysis against deionized water. The dialysate was passed through a filter (0.45 μm-sized pores), producing clear brownish-yellow solution as a result. It was stored at a temperature of 10 °C, protected from light [16].

The organic precursor was prepared according to a procedure similar to that described in [19]; 3-methyl-1-phenyl-4-formyl-pyrazole-5-one (2 mmol) was dissolved in 96% ethanol (25 ml) by stirring and heating. The corresponding 4-chlorobenzoic acid hydrazide (2 mmol) was added to the resulting solution, which was then stirred and heated for 1–2 h until a precipitate formed. The precipitate was left in mother liquor for a long time (overnight); then it was filtered off, washed with ethanol and dried in air. Target product (weighing 680 mg) was obtained with a yield of 96% by this procedure.

Solutions were prepared for each of the starting materials (IMPH and $C_{60}$) as active layers were formed. Chloroform was used as solvent for the IMPH compound, and dichloromethane for powder $C_{60}$ (in concentrations of 0.5 mg/ml). There was no need to use additional solvent to prepare the FWS samples. The final stage of sample preparation started after the obtained suspensions were held at room temperature for at least 48 h. This stage consisted in simultaneously depositing aged suspensions (1 ml each) on substrates intended for measurements in the given frequency ranges.

The following notations were introduced for the film samples:

*IMPH* (N-isoamylisatin 4-methylphenylhydrazone) refers to the samples precipitated on glass from N-isoamylisatin 4-methylphenylhydrazone solutions in chloroform;

*FFWS* (fullerene from fullerene water system) to the samples precipitated from aqueous solutions of $C_{60}$;

*FDCM* (fullerene from dichloromethane) to the samples precipitated from dichloromethane suspensions.

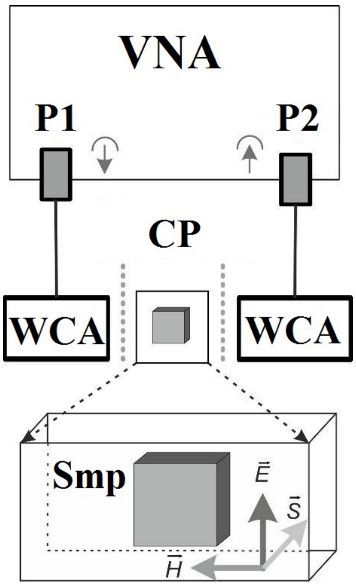


Fig. 1. Block diagram of measurements in waveguide: VNA is the vector circuit analyzer P4226; P1, P2 are the input and output contacts (ports); WCA are the coaxial waveguide transitions: CP is the calibration plane; Smp is the sample in the waveguide (microwave radiation vectors are shown)

## Interaction of microwave radiation with fullerene and IMPH films

We previously used the measuring system including the P4226 vector analyzer (Fig. 1) to study the interaction of electromagnetic radiation with thin conducting and semiconducting films [20]. Since the main difficulty in measuring the characteristics of semiconductor fullerene ($C_{60}$) and organic (IMPH) films was their high ohmic resistance due to small thickness, the measuring system had to be highly sensitive, requiring fine tuning. Measurements were carried out in a closed waveguide in the 2.5–4.0 and 8.2–12.0 GHz ranges to minimize external interference. Through-Reflect-Line calibration was performed to compensate for coaxial waveguide transitions and other interfering factors, using a reflection measure and a quarter-wave line, which yielded fairly accurate results. The effective area of interaction of radiation with the samples was 10% of the cross-sectional area of the waveguide, which helped avoid capacitive and inductive effects from the test sample on the measuring system. The samples were placed in the geometric center of the waveguide cross-section (see Fig. 1) and fixed using a dielectric substrate made from a material that was transparent to microwave radiation. Thus, the sample was at maximum electric field during measurements; since the fundamental mode $H_{10}$ was used, it can be argued that the area of the sample accounted for the largest part of the energy.

The actual interaction of microwave radiation with the samples was determined by the matrix of $S$ parameters taking into account the main components $S_{21}$ and $S_{11}$, corresponding to the radiation directly incident from the first port P1. The initial measurements indicated that the properties of the waveguide with the given structure are close to the properties of a reciprocal two-port network, i.e., the gain is the same in both directions. In view of this, we used the main components $S_{21}$ and $S_{11}$ corresponding to direct incidence from the first port of the VNA.

Recall that the components of $S$ parameters are the voltage ratios of the reflected ($V_{ref}$), incident ($V_{inc}$) and transmitted ($V_{trans}$) radiation, i.e.,

$$S_{11} = \frac{V_{ref}}{V_{inc}} \text{ and } S_{21} = \frac{V_{trans}}{V_{inc}};$$

while the powers of the transmitted ($P_{trans}$) and reflected ($P_{ref}$) waves are expressed as

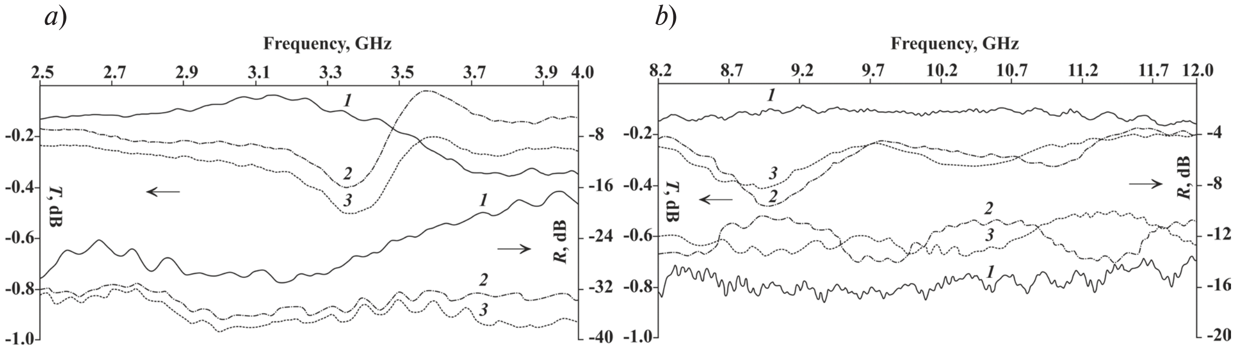


Fig. 2. Frequency spectra of FFWS (*1*), IMPH (*2*) and FDCM (*3*) samples exposed to microwave radiation in 2.5–4.0 (*a*) and 8.2–12.0 (*b*) GHz ranges;
*T*, *R* are the coefficients of transmitted and reflected power, respectively

$$P_{trans} = \frac{|V_{trans}|^2}{Z_v};$$

$$P_{ref} = \frac{|V_{ref}|^2}{Z_v},$$

where $Z_v$ is the wave impedance.

We first determined the coefficients of transmitted (*T*) and reflected (*R*) power, and then calculated the absorption coefficient *A* (Fig. 2):

$$T = \frac{P_{trans}}{P_{inc}} = \frac{|V_{trans}|^2}{|V_{inc}|^2} = |S_{21}|^2;$$

$$R = \frac{P_{ref}}{P_{inc}} = \frac{|V_{ref}|^2}{|V_{inc}|^2} = |S_{11}|^2;$$

$$A = 1 - |S_{11}|^2 - |S_{21}|^2.$$

Irregular frequency characteristics of the transmission and reflection coefficients confirm our above assumption that the interaction of radiation with thin carbon and organic films has a complex nature. However, the obtained dependences can provide a simplistic explanation for the specific effect of internal structure of the films on the electromagnetic wave. For this reason, we selected the characteristic frequencies $\nu_1$ = 3.4 GHz and $\nu_2$ = 9.1 GHz, at which dips are observed in the frequency dependences of transmittance, for detailed analysis of each of the given spectral ranges (see Fig. 2). In other words, the two materials (IMPH and FDCM) exhibited attenuation of electromagnetic waves at these frequencies. Moreover, the respective curves are similar for both the reflected power and the transmittance at frequencies $\nu_1$ and $\nu_2$. However, maximum transmittance is observed for these structures at frequencies of approximately 3.6 GHz. It is also worth noting that the spectrum is quite uniform and only at these frequencies are anomalies observed, which is obviously due to the specific structure of the material under study. In addition, the reflection and transmission coefficients do not behave anti-symmetrically (curves *2* and *3* in Fig. 2, *a*), suggesting that microwave radiation is absorbed.In contrast to the behavior of IMPH and FDCM samples exposed to microwave radiation, FFWS samples did not possess any pronounced characteristics. However, the samples exhibited an inverse trend to the behavior of other materials at frequencies of 2.5–4.0 GHz: namely, the transmission coefficient decreased with increasing frequency of the incident wave, and the reflection coefficient increased with decreasing transmission coefficient. This suggests that absorption of electromagnetic microwave waves is minimal, and the FFWS material itself has low electrical conductivity, which is, however, higher than that of the other two materials.

Analysis of the general frequency characteristics of the given films led us to conclude that the relationship of the absorbed wave energy with the film volume should be taken into account. The transmission minima at 3.32 and 8.97 GHz were examined more closely. The specific absorbed power *Q* was calculated as the ratio of the power $P_{abs}$ absorbed by the sample to its volume *V*, i.e., *a*) *b*)

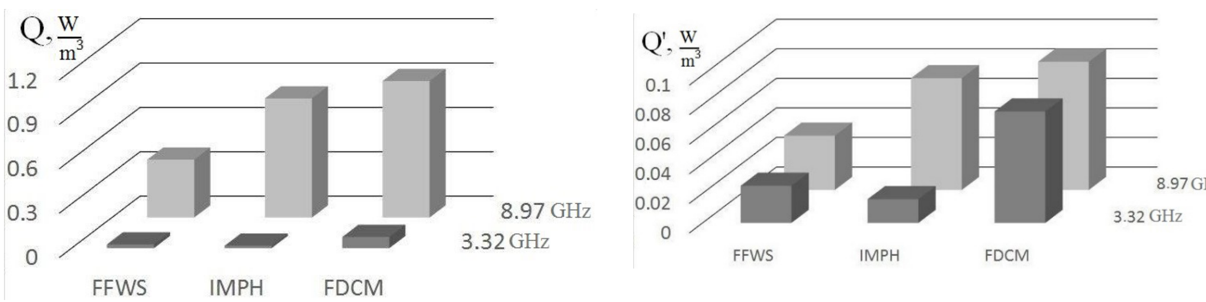


Fig. 3. Graphical representation of specific absorbed microwave power for FFWS, IMPH, and FDCM film samples calculated by Eqs. (1) (*a*) and (2) (*b*)

$$Q = P_{abs}/V, \tag{1}$$

and $P_{abs}$ was calculated as the product of the output power $P_{inc}$ of the VNA generator, equal to −10.00 dBm, multiplied by absorption coefficient $A$:

$$P_{abs} = P_{inc}\left(1 - \left|S_{11}\right|^2 - \left|S_{21}\right|^2\right).$$

The volume $V$ was found by averaging the film thicknesses, which we measured using a LOMO MII-4M interference microscope in the most characteristic segments of the samples.

Comparing the specific absorbed power for three samples (Fig. 3, *a*), we found that FDCM films have the highest absorptivity. The lowest absorptivity at 3.32 GHz was observed for IMPH samples, while FFWS films had the lowest absorptivity at 8.97 GHz. Notably, microwave radiation had a constant power at the output of the P4226 generator, so it was impossible to accurately compare the absorptivity of the films at different frequencies. For example, the specific absorbed power was higher at 8.97 GHz than at 3.32 GHz. This effect is not related to the properties of the given materials; it is explained by higher radiation density generated in a waveguide with a smaller cross section. To account for linear calculations, the results were normalized to compare different radiation densities. The normalized specific power (Fig. 3, *b*) obtained follows the expression

$$Q' = Q \cdot \frac{S_{23\times10}}{S_{72\times34}}, \tag{2}$$

where $S_{23\times10}$, $S_{23\times10}$ are the cross-sectional areas of the corresponding waveguide lines.

Thus, the dimensions of the waveguides are taken into account here.

**Midwave-IR absorption spectra**

The interaction of midwave optical radiation with heterostructure elements was studied with an Agilent Cary 630 FTIR spectrometer in the range of spatial frequencies from 650 to 4000 cm$^{-1}$, corresponding to direct spectrum of 19.48–119.92 THz, with a resolution of 110 GHz (4 cm$^{-1}$). The interaction of infrared electromagnetic waves with IMPH, FDCM and FFWS films was particularly pronounced in the frequency ranges of 20–50 and 78–108 THz (667–1667 cm$^{-1}$ and 2601–3602 cm$^{-1}$).

While the smoothest spectrum for the interaction of microwave radiation with film structures was observed for FFWS samples, the FDCM structures had the smallest number of peaks in the IR range. In particular, a range of relatively narrow absorption bands was observed for the lower frequency range of 20–50 THz (667–1667 cm$^{-1}$). For example, the peaks observed for FDCM samples at 41.07 and 43.68 THz (1369 and 1457 cm$^{-1}$) corresponded to the $C_{sp3}$–H bond, and the peaks at 35.46 and 42.81 THz (1182 and 1427 cm$^{-1}$) to $C_{60}$, with the last band coinciding with the band from the alkyl group at 43.68 THz (1456 cm$^{-1}$) (Fig. 4, *a*). Two characteristic narrow IR absorption bands are clearly seen for FFWS films at 35.43 and 42.81 THz (1181 and 1427 cm$^{-1}$) (due to C–C bonds) of $C_{60}$molecules, although they partially overlap with other bands. Absorption bands in the range of 49.46–49.76 THz (1649–1659 cm$^{-1}$) (due to the C=O bond) for the amide carbonyl group and 29.98–32.97 THz (1000–1099 cm$^{-1}$) are characteristic for vibrations of the C–O group. In this case, there are no bands characteristic for amino acids (see Fig. 4, *a*). The frequency spectrum of IR absorption by IMPH films is characterized by a significant number of peaks, which is due to numerous chemical bonds in the of N-isoamylisatin 4-methylphenylhydrazone molecule (see Fig. 4, *a*). Peaks characteristic for vibrations of C=O and C=N atomic groups are found at frequencies of 46.7 and 50.12 THz (1557 and 1671 cm$^{-1}$). Stretching vibrations of benzene rings play the main role in the frequency range of 40.89–48.26 THz (1363–1609 cm$^{-1}$). A sequence of absorption maxima is found in the frequency range of 31.59–38.82 THz (1053–1294 cm$^{-1}$) due to bending and stretching vibrations of C–N, C–C and C–H groups. The main role in the frequency range of 22.30–33.81 THz (743–1127 cm$^{-1}$) is played by bending vibrations of C–H groups in benzene rings and in the alkyl substituent.

The spectrum is not so diverse at higher frequencies (Fig. 4, *b*), characterized mainly by absorption peaks at frequencies of 75–90 THz (2501–3002 cm$^{-1}$). In particular, a double peak observed in the range of 83–89 THz (2768–2968 cm$^{-1}$) for films precipitated from dichloromethane solution, which can be attributed to $C_{sp3}$–H vibrational modes, appears as a wider single peak for FFWS films (Fig. 4, *b*). However, this peak also has a relatively long absorption band at 90–108 THz (3002–3602 cm$^{-1}$) with a maximum at 100 THz (3335 cm$^{-1}$). A series of absorption bands associated with vibrations of the N–H and C–H groups were observed for the IMPH sample in the frequency range of 85.7–101.9 THz (2858–3398 cm$^{-1}$), (see Fig. 4, *b*).

### Microscopy of film surface

Geometry of the surface exposed to such high frequencies of electromagnetic radiation plays an important role, so each of the individual elements and the film as a whole (i.e., the IMPH, FDCM, FFWS compounds) were monitored by reflection and transmission microscopy using a LOMO MII-4M microinterferometer, with enhanced light via a semiconductor laser and with an elongated optical path to a camera with a 1/2 FF 10 MP sensor.

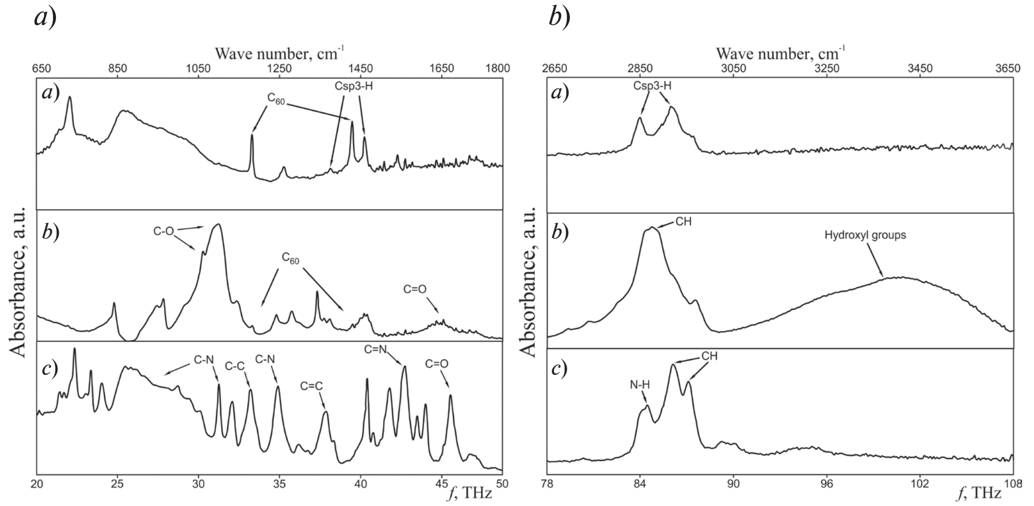


Fig. 4. IR optical absorption spectra of FDCM (*1*), FFWS (*2*) and IMPH (*3*) film samples in 667–1667 cm$^{-1}$ (*a*) and 2601–3602 cm$^{-1}$ (*b*) frequency ranges

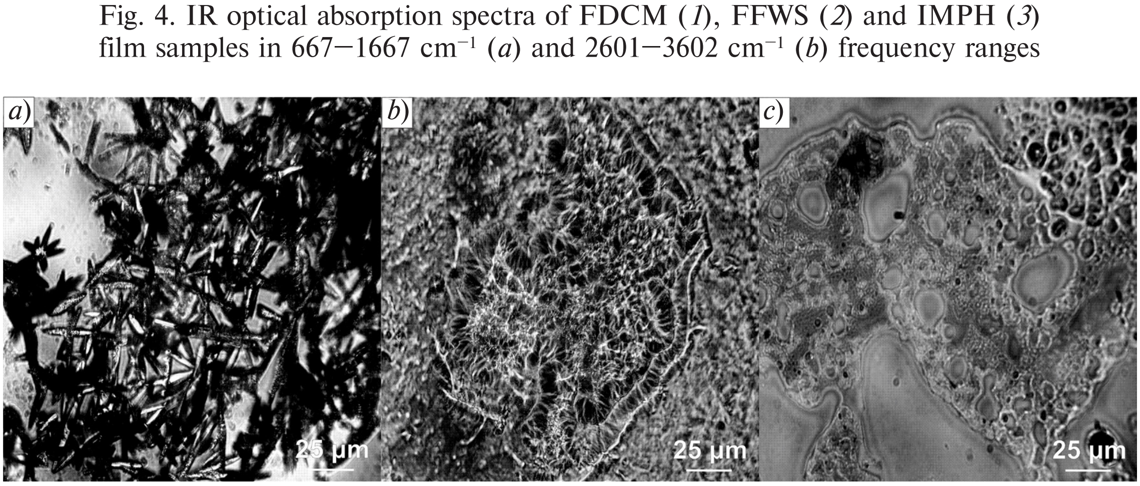


Fig. 5. Micrographs of nanostructured FDCM (*a*), FFWS (*b*) and IMPH (*c*) films

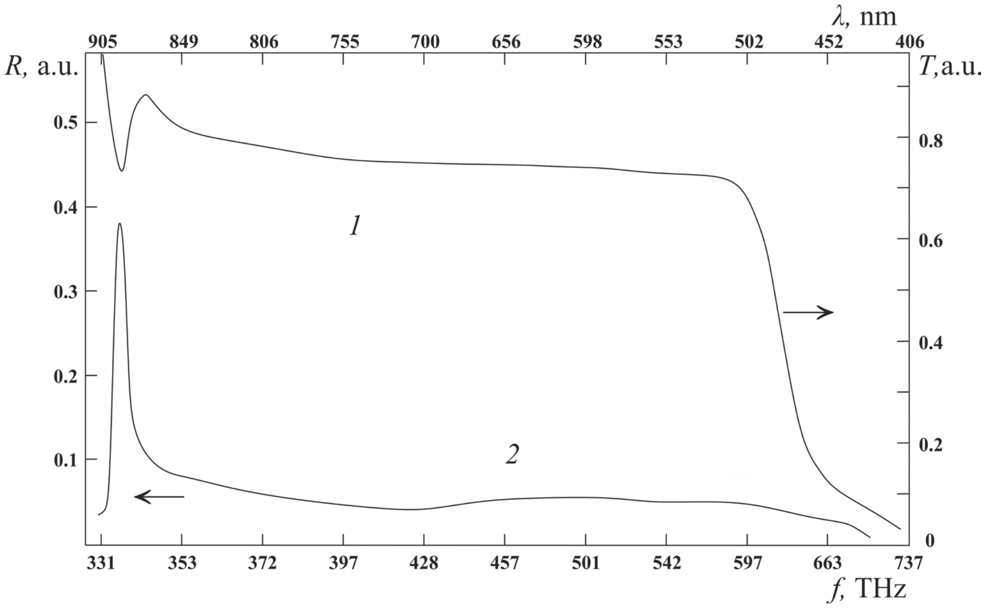


Fig. 6. Optical transmission (*1*) and reflection (*2*) spectra of IMPH thin film in 406–909 nm range

We should note that the surfaces of nanostructured films are irregular, characterized by pronounced separate structures or even regions (Fig. 5). The most characteristic fragments of FDCM, FFWS and IMPH film surfaces are shown.

Distinct microstructures shaped as three-dimensional stars were observed for films precipitated from solution of fullerene in dichloromethane (FDCM), The sizes of individual structures reached 16–20 μm, while film thickness averaged 400–500 nm (see Fig. 5, *a*). FFWS film samples had a fairly uniform surface with localized hexagonal structures. The sizes of individual structures reached 50–80 μm, while film thickness aviaveraged 1.8 μm (see Fig. 5, *b*). The surface of hydrazone films (IMPH) is also relatively uniform, which is explained by considerable length of the 4-methylphenylhydrazone N-isoamylisatin molecule and, in particular, the amyl radical. The film thickness was 1.8–2.0 μm (see Fig. 5, *c*).

## Optical transmission and reflection spectra in the visible range

A prism monochromator with an IR filter and a halogen lamp was used for collecting the transmission and reflection spectra of the given films. The spectrometer was calibrated for hydrogen radiation before each series of experiments. A clean substrate was used as a normalizing basis.

FDCM films had the highest absorption: their linear transmission spectrum was at the level of photomultiplier noise and was practically zero. The reflected component was absent for these films. While FFWS samples had similar spectral characteristics, they exhibited a slight dip in the short-wave part of the spectrum.

The optical spectra of light transmission through IMPH films were characterized by sharp minima in the near IR region at 336.85 and 340.68 THz (890 and 880 nm). Accordingly, sharp maxima were observed in the reflection

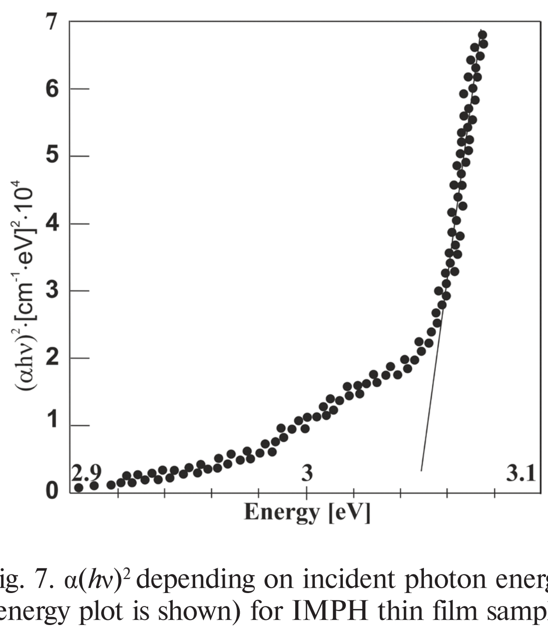


Fig. 7. $\alpha(h\nu)^2$ depending on incident photon energy (energy plot is shown) for IMPH thin film sample

spectra, along with a general decrease in the high-frequency region of 599.6–713.8 THz (500–420 nm) due to absorption in the film (Fig. 6).

We calculated the logarithm of the ratio of transmission coefficient $T$ and reflection coefficient $R$ for the given sample thickness, with subsequent linearization (Fig. 7) with a constant for indirect allowed transitions ($m$ = 2) [21]. The formula

$$\alpha h\nu = A\left(h\nu - E_g\right)^m, \tag{3}$$

was used for the calculations, where α is the absorption coefficient, $A$ is a constant, $h\nu$ is the optical photon energy, $E_g$ is the band gap of the film material.

As a result of the calculations, we obtained the band gap value for the IMPH compound: $E_g$ = 3.05 eV.

### Conclusion

Almost all film samples of IMPH, FDCM, and FFWS reacted noticeably to electromagnetic radiation in a wide frequency range, i.e., absorption or reflection of incident energy. The infrared region turned out to be the most inhomogeneous the in the range of 20–50 THz (667–1667 cm$^{-1}$), where a series of narrow-band peaks was observed, with the narrowest bands reaching several hundred gigahertz.

The given structures were less sensitive to microwave radiation. Notably, however, a dip in the transmittance curve was observed at frequencies of 3.4 and 9.1 GHz for the samples precipitated from fullerene suspensions in dichloromethane (FFWS) and from N-isoamylisatin 4-methylphenylhydrazone in chloroform (IMPH).

Sharp minima were observed in the visible absorption spectra at 336.85 and 340.68 THz (890 and 880 nm), accompanied by general decrease in energy in the range of 599.6–713.8 THz (500–420 nm) for IMPH films. Analyzing the obtained experimental data, we have concluded that FDCM films had the highest absorption in all three ranges of electromagnetic radiation considered.

Thus, interaction of electromagnetic radiation with carbon and organocarbon materials can take diverse forms, requiring comprehensive experimental and theoretical studies. We are confident even at this stage that the behavior of microwave, optical absorption and reflection spectra can be controlled by synthesizing complex molecular complexes serving as a basis for heterostructural transitions for experiments in the given frequency ranges.

### Acknowledgment

We wish to express our gratitude to the staff of $S_{60}$Bio (Skolkovo, Moscow) for providing us with a sample of water-soluble fullerene.

The study was financially supported by the Russian Foundation for Basic Research as part of scientific project no. 19-32-90038.

## REFERENCES

1. **Kemp S.,** Global digital statshot, URL: https://wearesocial.com/global-digital-report-2019.

2. **Rout S.P.,** 5th generation mobile technology – a new milestone to future wireless communication networks, International Journal of Science and Research. 5 (5) (2016) 529–534.

3. **Kumar A., Gupta M.,** A review on activities of fifth generation mobile communication system, Alexandria Engineering Journal. 57 (2) (2018) 1125–1135.

4. **Baimova J.A., Korznikova E.A., Dmitriev S.V., et al.,** Review on crumpled graphene: unique mechanical properties, Reviews on Advanced Materials Science. 39 (1) (2014) 69–83.

5. **Lebedeva O.S., Lebedev N.G.,** The influence of the stretching and compression deformations on the piezoresistance of the carbon nanotubes and graphene nanoribbons, St. Petersburg State Polytechnical University Journal. Physics and Mathematics (1 (189)) (2014) 26–34.

6. **Eletskii** A.V., Mechanical properties of carbon nanostructures and related materials, Phys. Usp. 50 (3) (2007) 225–261.

7. **Li Y., Liu S., Sun J., et al.,** Effects of the oxygen content of reduced graphene oxide on the mechanical and electromagnetic interference shielding properties of carbon fiber/reduced graphene oxide-epoxy composites. New Carbon Materials. 34 (5) (2019) 489–498.

8. **Wang X., Jiang H.T., Yang K.Y., et al.,** Carbon fiber enhanced mechanical and electromagnetic absorption properties of magnetic graphene-based film, Thin Solid Films. 674 (31) (2019) 97–102.

9. **Chen F.C., Chu C.W., He J., et al.,** Organic thin-film transistors with nanocomposite dielectric gate insulator. Applied Physics Letters. 85 (15) (2004) 3295–3297.10. **Gusev A.N., Kiskin M.A., Braga E.V., et al.,** Novel zinc complex with an ethylenediamine schiff base for high-luminance blue fluorescent OLED applications, The Journal of

Physical Chemistry. 123 (18) (2019) 11850–11859.

11. **Ziminov V.M., Zakharova I.B.,** The rectifying properties of C60 fullerene-based structures, St. Petersburg State Polytechnical University Journal. Physics and Mathematics (2 (146)) (2012) 18–21.

12. **Gusev A.N., Mazinov A.S., Tyutyunik A.S., Gurchenko V.S.** Spectral and conductive properties of film heterostructures based on fullerene-containing material and 4-methylphenylhydrazone N-isoamilisatine; Radio Electronics, Nanophysics and Information Technologies. 11 (3) (2019) 331–336.

13. **Konenkamp R., Priebe G., Pietzak B.,** Carrier mobilities and influence of oxygen in C60 films, Physical Review B. 60 (16) (1999) 11804–11808.

14. **Tapponnier A., Biaggio I., Gunter P.,** Ultrapure $C_{60}$ field-effect transistors and the effects of oxygen exposure, Applied Physics Letters. 86 (11) (2005) 112114.

15. **Gusev A.N., Mazinov A.S., Shevchenko A.I. et al.,** The voltage–current characteristics and photoelectric effect of fullerene $C_{60}$–N-isoamylisatin 4-methylphenylhydrazone heterostructures, Technical Physics Letters. 45 (10) (2019) 997–1000.

16. **Andreev S.M., Purgina D.D., Bashkatova E.N., et al.,** Facile preparation of aqueous fullerene $C_{60}$ nanodispersions, Nanotechnol. Russia. 9 (7–8) (2014) 369–379.

17 **Mazinov A.S., Gurchenko V.S., Tyutyunik A.S., Shevchenko A.I.,** Influence of structural features of fullerene-containing material on its resistive properties, Ecological Bulletine of the Black Sea Economic Cooperation. 15 (2) (2018) 86–93.

18. **Mazinov A.S., Gurchenko V.S., Tyutyunik A.S., Shevchenko A.I.,** Influence of structural features of fullerene-containing material deposited from solution on its resistive properties, Ecological Bulletine of the Black Sea Economic Cooperation. 15 (4) (2018) 85–92.

19. **Cigan M., Jakusova K., Gaplovsky M., et al.,** Isatin phenylhydrazones: anion enhanced photochromic behavior, Photochemical and Photobiological Sciences. 14 (11) (2015) 2064–2073.

20. **Starostenko V.V., Mazinov A.S., Fitaev I.S., et al.,** Forming surface dynamics of conductive aluminum films deposited on amorphous substrates, Prikladnaya Phyzika. (4) (2019) 60–65.

21. **Al-Saidi I., Sadik F.,** Synthesis and investigation of phenol red dye doped polymer films, Advances in Materials Physics and Chemistry. 6 (5) (2016) 120–128.

*Received 18.01.2020, accepted 14.02.2020.*

## THE AUTHORS

**STAROSTENKO Vladimir V.**
*V.I. Vernadsky Crimean Federal University*
4 Vernadskogo Ave., Simferopol, 295007, Republic of Crimea, Russian Federation
starostenkovv@cfuv.ru

**MAZINOV Alim S-A.**
*V.I. Vernadsky Crimean Federal University*
4 Vernadskogo Ave., Simferopol, 295007, Republic of Crimea, Russian Federation
mazinovas@cfuv.ru

**TYUTYUNIK Andrey S.**
*V.I. Vernadsky Crimean Federal University*
4 Vernadskogo Ave., Simferopol, 295007, Republic of Crimea, Russian Federation
real-warez@mail.ru

**FITAEV Ibraim Sh.**
*V.I. Vernadsky Crimean Federal University*
4 Vernadskogo Ave., Simferopol, 295007, Republic of Crimea, Russian Federation
fitaev.i@cfuv.ru

**GURCHENKO Vladimir S.**
*V.I. Vernadsky Crimean Federal University*
4 Vernadskogo Ave., Simferopol, 295007, Republic of Crimea, Russian Federation
gurchenko_v@mail.ru

## СПИСОК ЛИТЕРАТУРЫ


1. **Kemp S.** Global digital statshot. Режим доступа: https://wearesocial.com/global-digital-report-2019 (дата обращения: 10.01.2020).

2. **Rout S.P.** 5th generation mobile technology – a new milestone to future wireless communication networks // International Journal of Science and Research. 2016. Vol. 5. No. 5. Pp. 529–534.

3. **Kumar A., Gupta M.** A review on activities of fifth generation mobile communication system // Alexandria Engineering Journal. 2018. Vol. 57. No. 2. Pp. 1125–1135.

4. **Baimova J.A., Korznikova E.A., Dmitriev S.V., Liu B., Zhou K.** Review on crumpled graphene: unique mechanical properties// Reviews on Advanced Materials Science. 2014. Vol. 39. No. 1. Pp. 69–83.

5. **Лебедева О.С., Лебедев Н.Г.** Влияние деформаций растяжения и сжатия на пьезорезистивность углеродных нанотрубок и графеновых нанолент // Научно-технические ведомости СПбГПУ. Физико-математические науки. 2014. № 1 (189). С. 26–34.

6. **Елецкий А.В.** Механические свойства углеродных наноструктур и материалов на их основе // Успехи физических наук. 2007. Т. 177. № 3. С. 233–274.

7. **Li Y., Liu S., Sun J., Li S., Chen J., Zhao Y.** Effects of the oxygen content of reduced graphene oxide on the mechanical and electromagnetic interference shielding properties of carbon fiber/reduced graphene oxide-epoxy composites // New Carbon Materials. 2019. Vol. 34. No. 5. Pp. 489 – 498.

8. **Wang X., Jiang H.T., Yang K.Y., Ju A.X., Ma C.Q., Yu X.L.** Carbon fiber enhanced mechanical and electromagnetic absorption properties of magnetic graphene-based film // Thin Solid Films. 2019. Vol. 674. No. 31. Pp. 97–102.

9. **Chen F.C., Chu C.W., He J., Yang Y., Lin J.L.** Organic thin-film transistors with nanocomposite dielectric gate insulator // Applied Physics Letters. 2004. Vol. 85. No. 15. Pp. 3295–3297.

10. **Gusev A.N., Kiskin M.A., Braga E.V., et al.** Novel zinc complex with an ethylenediamine schiff base for high-luminance blue fluorescent OLED applications // The Journal of Physical Chemistry. 2019. Vol. 123. No. 18. Pp. 11850–11859.

11. **Зиминов В.М., Захарова** И.Б. Выпрямляющие свойства структур на основе фуллерена $C_{60}$ // Научно-технические ведомости СПбГПУ. Физико-математические науки. 2012. № 2 (146). С. 18–21.

12. **Gusev A.N., Mazinov A.S., Tyutyunik A.S., Gurchenko V.S.** Spectral and conductive properties of film heterostructures based on fullerene-containing material and 4-methylphenylhydrazone N-isoamilisatine // Radio Electronics, Nanophysics and Information Technologies. 2019. Vol. 11. No. 3. Pp. 331–336.

13. **Konenkamp R., Priebe G., Pietzak B.** Carrier mobilities and influence of oxygen in $C_{60}$ films // Physical Review B. 1999. Vol. 60. No. 16. Pp. 11804–11808.

14. **Tapponnier A., Biaggio I., Gunter P.** Ultrapure $C_{60}$ field-effect transistors and the effects of oxygen exposure // Applied Physics Letters. 2005. Vol. 86. No. 11. P. 112114.

15. **Гусев А.Н., Мазинов А.С., Шевченко А.И., Тютюник А.С., Гурченко В.С., Брага Е.В.** Вольтамперные характеристики и фотоэлектрический эффект гетероструктур фуллерен $C_{60}$ – 4-метилфенилгидразон N-изоамилизатина // Письма в ЖТФ. 2019. Т. 45. № 19. С. 40–43.

16. **Андреев С.М., Пургина Д.Д., Башкатова Е.Н.,** Гаршев **А.В.,** Маерле **А.В., Хаитов М.Р.** Эффективный способ получения водных нанодисперсий фуллерена $C_{60}$ // Российские нанотехнологии. 2014. № 7–8 (9). С. 24–30.

17. **Мазинов А.С., Работягов К.В., Гурченко** В.С., Тютюник **А.С** Влияние структурных особенностей фуллеренсодержащего материала на его резистивные свойства // Экологический вестник научных центров Черноморского экономического сотрудничества. 2018. Т. 2 № .15. С. 93–86.

18. **Мазинов А.С., Гурченко** В.С., Тютюник **А.С., Шевченко А.И.** Влияние структурных особенностей фуллеренсодержащего материала на его резистивные свойства при осаждении из раствора // Экологический вестник научных центров Черноморского экономического сотрудничества. 2018. Т. 15. № 4. С. 85–92.

19. **Cigan M., Jakusova K., M. Gaplovsky M., Filo J., Donovalova J., Gaplovsky A.** Isatin phenylhydrazones: anion enhanced photochromic behavior// Photochemical and Photobiological Sciences. 2015. Vol. 14. No. 11. Pp. 2064–2073.

20. **Старостенко В.В., Мазинов А.С., Фитаев И.Ш., Таран Е.П.,** Орленсон **В.Б.** Динамика формирования поверхности проводящих пленок алюминия на аморфных подложках // Прикладная физика. 2019. № 4. С. 60–65.

21. **Al-Saidi I., Sadik F.** Synthesis and investigation of phenol red dye doped polymer films // Advances in Materials Physics and Chemistry. 2016. Vol. 6. No. 5. Pp. 120–128.


*Статья поступила в редакцию 18.01.2020, принята к публикации 14.02.2020.*

## СВЕДЕНИЯ ОБ АВТОРАХ

**СТАРОСТЕНКО Владимир Викторович** – доктор физико-математических наук, заведующий кафедрой радиофизики и электроники Крымского федерального университета имени В.И. Вернадског.

295007, Российская Федерация, Республика Крым, г. Симферополь, пр. Академика Вернадского, 4

starostenkovv@cfuv.ru

**МАЗИНОВ Алим Сеит-Аметович** – кандидат технических наук, доцент кафедры радиофизики и электроники Крымского федерального университета имени В.И. Вернадского.

295007, Российская Федерация, Республика Крым, г. Симферополь, пр. Академика Вернадского, 4

mazinovas@cfuv.ru

**ТЮТЮНИК Андрей Сергеевич** – аспирант кафедры радиофизики и электроники Крымского федерального университета имени В.И. Вернадского.

295007, Российская Федерация, Республика Крым, г. Симферополь, пр. Академика Вернадского, 4

real-warez@mail.ru

**ФИТАЕВ Ибраим Шевкетович** – ведущий специалист кафедры радиофизики и электроники Крымского федерального университета имени В.И. Вернадского.

295007, Российская Федерация, Республика Крым, г. Симферополь, пр. Академика Вернадского, 4

fitaev.i@cfuv.ru

**ГУРЧЕНКО Владимир Сергеевич** – аспирант кафедры радиофизики и электроники Крымского федерального университета имени В.И. Вернадского.

295007, Российская Федерация, Республика Крым, г. Симферополь, пр. Академика Вернадского, 4

gurchenko_v@mail.ru